IOSR Journal of Mechanical and Civil Engineering (IOSR-JMCE)
ISSN: 2278-1684, PP: 01-15
www.iosrjournals.org

Active Thrust on an Inclined Wall under the Combined Effect of Surcharge and Self- Weight

D. M. Dewaikar*, Jagabandhu Dixit †, S. R. Pandey ◦ and P.R.Mutgi+

** Emeritus Fellow, Indian Institute of Technology Bombay, Mumbai, India, PIN – 400076*
† Research Scholar, Indian Institute of Technology Bombay, Mumbai, India, PIN – 400076
◦ Former Post Graduate Student, Indian Institute of Technology Bombay, Mumbai, India, PIN – 400076
+Principal, J. J. Magdum College of Engineering, Jaisingpur, India, PIN - 416101

ABSTRACT: *Active thrust and its point of application depend upon a combination of several parameters such as angles of wall friction, soil internal friction, backfill slope and wall back. A method based on the principle of superposition along with the conditions of equilibrium is used in the present analysis to determine the active thrust and its point of application for an inclined wall retaining horizontal cohesionless backfill under the combined effect of surcharge and self-weight. Coulomb's failure mechanism along with Kötter's equation is used to determine the distribution of soil reaction and its point of application on the failure surface.*
Keywords Kötter's equation, point of application, active thrust, self-weight, surcharge effect

1. INTRODUCTION

In many applications of geotechnical engineering, the evaluation of active earth pressure is required for the design of retaining wall, basement wall and sheet pile etc. The classical solutions of lateral earth pressure are provided by Coulomb (1776) and Rankine (1857). These fundamental solutions still form the basis of earth pressure calculations today. Coulomb (1776) first studied the earth pressure problem using the limit equilibrium method. His theory considers the stability of a wedge of soil between a retaining wall and the failure plane. It is well verified for the frictional soil in active state; but it is not the case for either the cohesive soil or for the passive states. The point of application of active thrust is assumed at a distance of one-third of the height of the wall from its base and independent of various parameters such as soil friction angle, ϕ, angle of wall friction, δ, backfill angle, β, and wall inclination angle. Caquot and Kerisel (1948) presented tables of active earth pressure coefficients derived from a method which directly integrates the equilibrium equations along the combined planer and logarithmic spiral failure surfaces. Janbu (1957) extended the generalized procedure of slices of slope stability analysis for the computation of active earth pressure coefficients on a vertical wall, retaining horizontal cohesionless backfill. In this method, assumptions regarding the line of action of thrust through the lower third of each slices and overall equilibrium are made. Sokolovski (1960) used finite difference approach to analyze the lateral earth pressures.

Rahardjo and Fredlund (1983) used the method of slices for computing active pressure coefficients in respect of a cohesionless soil by considering the soil mass in the state of limit equilibrium. Kerisel and Absi (1990) proposed a log spiral failure surface and presented their results in the form of charts. Ching and Sao (1994) used discrete element analysis for active and passive pressure distribution on the retaining wall. Chen and Li (1998) used the method of slices for computing active earth pressure coefficients in respect of a cohesionless soil by considering the soil mass in the state of limit equilibrium. Calculations of lateral earth pressure using the method proposed by Wang (2000) do not consider suitable earth pressure coefficients. His formulation cannot be used to obtain the point of application of the active thrust. Lancellotta (2002) provided an analytical solution for the active earth pressure coefficients, based on the lower bound theorem of plasticity. Soubra and Macuh (2002) used an approach based on rotational log-spiral failure mechanism with the upper-bound theorem of limit analysis for the active case. They evaluated earth pressure coefficients due to soil weight, vertical surcharge loading and soil cohesion for the case of an inclined wall and sloping backfill. Dewaikar and Halkude (2002) used Kötter's (1903) equation to determine the point of application of the active thrust (Coulomb, 1776) by taking moments of all the forces and reaction about the base of the retaining wall. Kame et al. (2010) proposed a method to determine the active earth pressure and its point of application on a vertical wall retaining horizontal cohesionless backfill with a log-spiral failure mechanism coupled with Kötter's

(1903) equation.

2. ACTIVE THRUST UNDER THE EFFECT OF SELF-WEIGHT OF SOIL

The active thrust, $P_{a\gamma}$ due to the self-weight of soil is obtained from the conditions of force equilibrium. Fig. 1 shows the free body diagram of the trial failure wedge with a plane failure surface (Coulomb, 1776). The soil wedge ABC is in equilibrium under the action of three forces: (1) self-weight, *W* of the trial soil wedge ABC, (2) the active thrust, $P_{a\gamma}$ at an angle δ to the normal on the back, and (3) the soil reaction, *R* along the face AB, at an angle ϕ to the normal on AB.

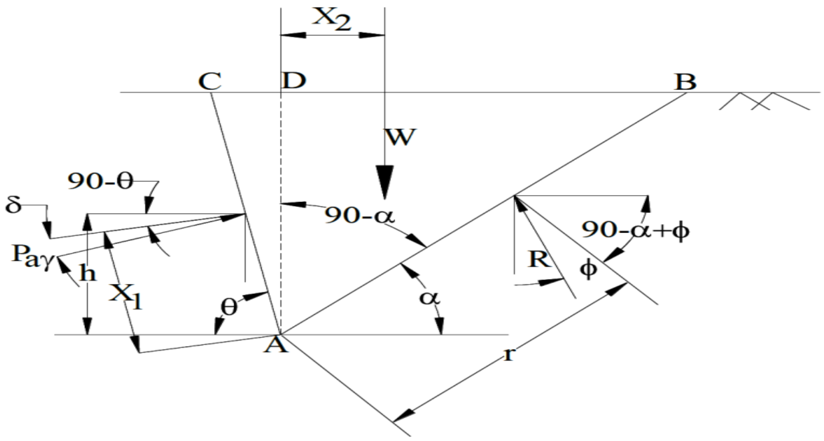

Fig. 1 Free body diagram of the trial wedge ABC

The symbols used in Fig. 1 are defined as follows $P_{a\gamma}$ =the active thrust

W = self-weight of the soil

R = soil reaction on the failure wedge

H = height of the retaining wall

h = height of point of application of active thrust from wall base

θ = inclination of the retaining wall with the horizontal

δ = friction angle between the wall and backfill soil

ϕ = soil friction angle

α = inclination of the trial failure plane with the horizontal

Using force equilibrium conditions, the active thrust $P_{a\gamma}$ is obtained corresponding to the critical value, α_{cr} of the angle

α.

3. SOIL REACTIVE PRESSURE ON THE FAILURE SURFACE DUE TO SELF-WEIGHT OF SOIL

This computation is facilitated using the Kötter's (1903) equation, which gives the distribution of reactive pressure on the failure surface, in a cohesionless soil medium and for the active state of equilibrium it is given as (Fig. 2).

$dp \quad 2p \tan \quad d_{cr} \quad \sin(\ _{cr} \quad)$

ds ds $—\,-$ $\phi \frac{\alpha}{\quad} = \gamma$ (1) $\alpha \quad -\phi$

Where,
dp = differential reactive pressure on the failure surface
ds = elemental length of the failure surface
α_{cr}= angle made by the tangent at the point of interest with the horizontal
=ϕ soil friction angle and
=γ soil unit weight

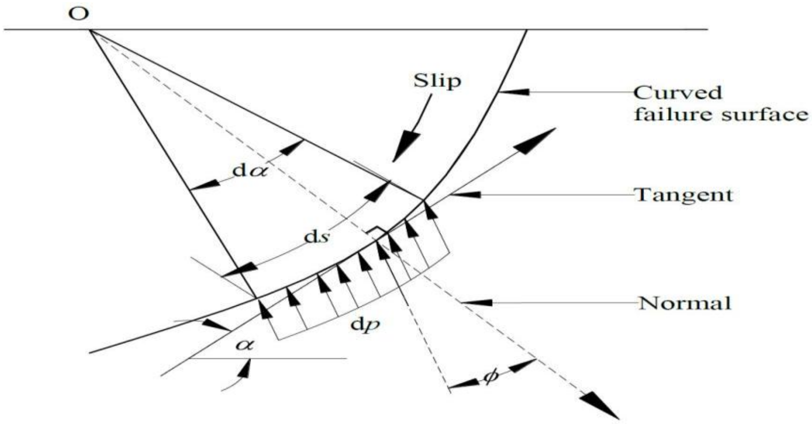

Fig. 2 Distribution of Reactive pressure on the failure surface

d cr

For a plane failure surface, $\frac{\alpha}{} =$

ds

and hence Eq. 1 can be written as,

$$\frac{dp}{ds} = \gamma \sin(\alpha_{cr} - \phi) \quad (2)$$

Integrating Eq. 2, the soil reactive pressure, *p* is given as,

$$p = \gamma \sin(\alpha_{cr} - \phi)s + c_1 \quad (3)$$

Where, the constant of integration, c_1 can be evaluated from the boundary condition. Pressure, *p* is zero at point B (Fig. 3), which corresponds to *s* =0, where, s represents the distance measured along the failure surface from point B. Hence, c_1 is zero and Eq. 3 becomes,

$$p = \gamma \sin(\alpha_{cr} - \phi)s \quad (4)$$

4. SOIL REACTION ON THE FAILURE PLANE DUE TO SELF-WEIGHT OF SOIL

The soil reaction, *R* on the failure plane can be obtained by the integration of the reactive pressure over the failure plane AB with proper limits. Hence the soil reaction, *R* can be expressed as,

$$R = \int_0^{AB} p\,ds \quad (5)$$

Substituting the value of *p* from Eq. 4 into Eq. 5, the soil reaction, *R* is obtained as,

$$R = \int_0^{AB} \gamma \sin(\alpha_{cr} - \phi)s\,ds \quad (6)$$

Integration of Eq. 6 with proper limits, the soil reaction, *R* is expressed as,

$$R = \frac{1}{2} AB^2 \gamma \sin(\alpha_{cr} - \phi) \quad (7)$$

Referring to Fig. 3, AB is obtained as,

$$AB = \frac{H}{\sin \alpha_{cr}} \quad (8)$$

Substituting the values of AB, from Eq. 8 into Eq. 7, the final expression of soil reaction, *R* on the failure surface is given as,

$$R = \frac{1}{2}\gamma H^2 \frac{\sin(\alpha_{cr} - \phi)}{\sin^2 \alpha_{cr}} \quad (9)$$

5. POINT OF APPLICATION OF REACTION ON THE FAILURE PLANE

This is computed by taking the moment of distribution of reaction about point A, (Fig. 3) and equating it to the moment of reaction, R about the same point.

$$R \cos\phi . r = \int_0^{AB} p.ds.(AB - s).\cos\phi \quad (10)$$

Or,

$$R.r = \int_0^{AB} p.ds.(AB - s) \qquad (11)$$

Where, *r* represents the distance of point of application of soil reaction, R from the base, A of the wall. Substituting the value of soil pressure, *p* from Eq. 4, and the above equation becomes,

$$R.r = \int_0^{AB} \gamma \sin(\alpha_{cr} - \phi) s (AB - s) ds \qquad (12)$$

Or,

$$R.r = \gamma \sin(\alpha_{cr} - \phi). \int_0^{AB} (AB.s - s^2).ds \qquad (13)$$

Integration yields,

$$R.r = \gamma. \sin(\alpha_{cr} - \phi). \frac{AB^3}{6} \qquad (14)$$

Now, substituting the value of soil reaction, *R* from Eq. 9 into the above equation gives,

$$\frac{1}{2}.AB^2.\gamma.\sin(\alpha_{cr} - \phi).r = \gamma.\sin(\alpha_{cr} - \phi).\frac{AB^3}{6} \qquad (15)$$

From which *r* is obtained as,

$$r = \frac{AB}{3} \qquad (16)$$

From Eq. 16 it is seen that, the soil reaction, *R* acts at a point, one-third the distance AB from point A (Fig. 3) and two-third the distance AB from ground surface along the failure surface.

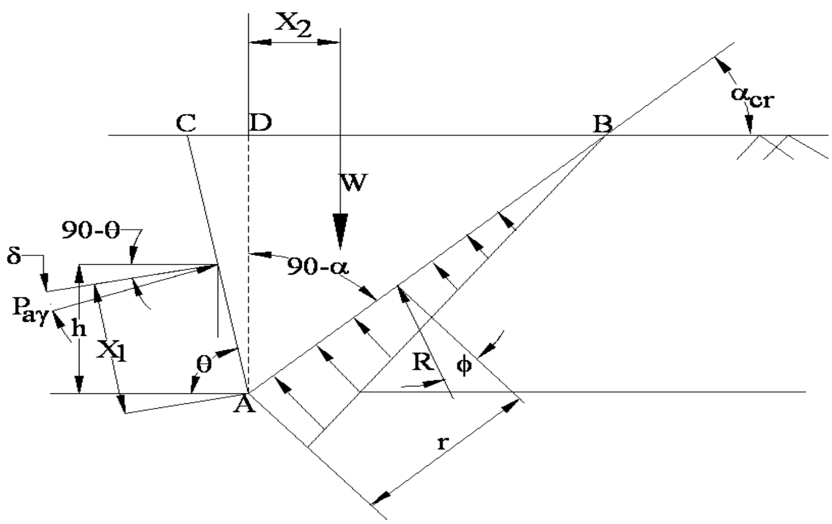

Fig. 3 Free body diagram of the failure surface

6. POINT OF APPLICATION OF ACTIVE THRUST DUE TO SELF-WEIGHT OF SOIL

After knowing the soil reaction, *R* and its point of application on the failure surface, moment equilibrium condition is applied to determine the point of application of the active thrust. Equating moments of all the forces and reactions about the base of the wall, at point A (Fig. 3)

$$P_{a\gamma}\cos\delta . X_1 = R\cos\phi . r - WX_2 \qquad (17)$$

From Eq. 17, the height of point of application of active thrust, $P_{a\gamma}$, due to self -weight of soil is given as (Fig. 3)

$$X_1 = \frac{R\cos\phi . r - WX_2}{P_{a\gamma}\cos\delta} \qquad (18)$$

The height of point of application of $P_{a\gamma}$ from the wall base, h is obtained as,

$$h = X_1 . \sin\theta \qquad (19)$$

The coefficient of active earth pressure ($K_{a\gamma}$) for the retaining wall with self-weight of soil is obtained as,

$$K_{a\gamma} = \frac{2P_{a\gamma}}{\gamma H^2} \qquad (20)$$

7. ACTIVE THRUST UNDER THE SURCHARGE EFFECT

Conditions of force equilibrium are used to determine the point of application of active thrust under surcharge effect. In Fig. 4 is shown an inclined retaining wall with horizontal cohesionless backfill under surcharge loading. The unit weight of the soil is not considered in the analysis. A trial failure plane (Coulomb, 1776) is considered, that meets the ground at an angle α with the horizontal. The trial wedge ABC is in equilibrium under the effect of three concurrent forces: (1) equivalent force of surcharge, (2) the active thrust, P_{aq}, at an angle δ to the normal on the back, and (3) The soil reaction, R at an angle to the normal on the trial failure surface AB.

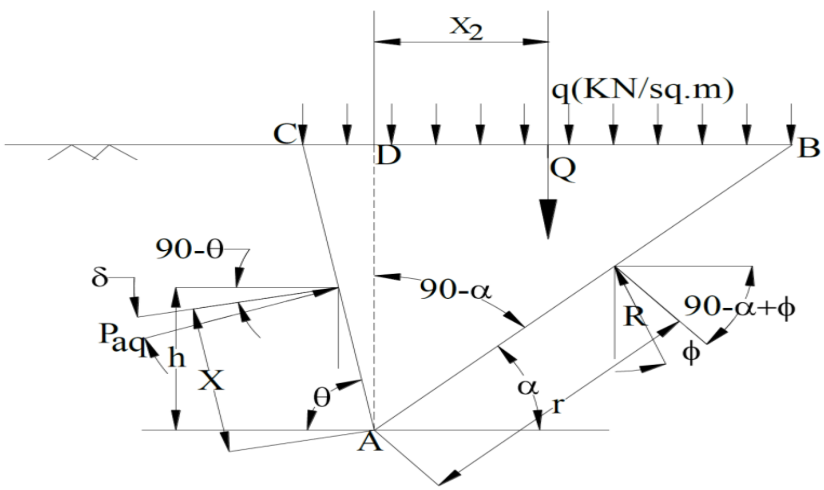

Fig. 4 Free body diagram of the trial failure wedge ABC

The relevant symbols used in Fig. 4 are defined as follows.

P_{aq} = active thrust

q = intensity of surcharge in kN/m^2

Q = equivalent force of the surcharge

The active thrust P_{aq} is obtained from the conditions of force equilibrium, corresponding to a critical value, α_{cr}, of the angle α, as given below.

$$P_{aq} = \frac{qH(\cot\theta + \cot\alpha_{cr})}{\cos(\theta-\delta) + \sin(\theta-\delta)\cot(\alpha_{cr}-\phi)} \qquad (21)$$

8 . SOIL REACTION ON THE FAILURE SURFACE

In this analysis γ=0 and with this condition, Eq. 1 can be written as

$$\frac{dp}{d\alpha_{cr}} = 2p\tan\phi \qquad (22)$$

$$dp = 2p\tan\phi . d\alpha_{cr} \qquad (23)$$

For a plane failure surface, $d\alpha_{cr}$ is zero and the corresponding solution is obtained as,

p = constant (24)

The above solution indicates that, soil reactive pressure p is uniformly distributed along the failure plane, AB. Therefore, the resultant soil reaction, R acts at the mid-point of the failure plane, AB (Fig. 5). The value of soil reaction, R on the failure surface is then obtained as,

$$R = \frac{qH(\cot\alpha_{cr} + \cot\theta)\sin(\theta-\delta)\sin\alpha_{cr}}{\sin(\alpha_{cr}-\phi)\sin(\alpha_{cr}-\beta)[\cos(\theta-\delta)+\sin(\theta-\delta)\cot(\alpha_{cr}-\phi)]} \qquad (25)$$

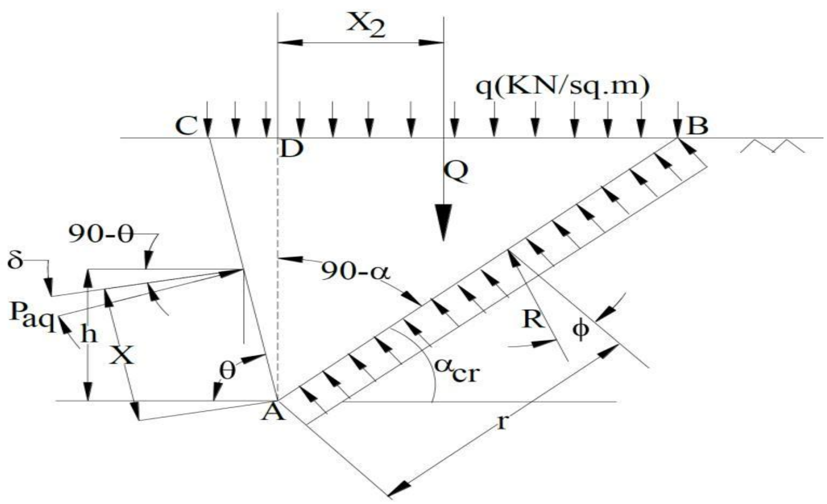

Fig. 5 Free body diagram of the failure wedge ABC

9. POINT OF APPLICATION OF ACTIVE THRUST DUE TO SURCHARGE EFFECT

$$\delta = \phi - \theta + \alpha \left[\frac{}{2\tan\alpha_{cr}} - \frac{}{2\tan\theta}\right]$$

In Fig. 5, X_2 is the distance of point of application of equivalent force, Q of surcharge from a vertical line passing through the base of the wall. A moment equilibrium condition is applied to determine the point of application of active thrust, P_{aq}. Taking moments of all the forces and reaction about the wall base, A, the following equation is obtained,

$$P_a \cos \quad 2 \quad .X \quad R\cos \quad .\frac{AB}{} \quad qH(\cot \quad \cot_{cr}) \quad H \qquad (26)$$

Substituting the values of soil reaction, *R* and active thrust, P_{aq} into Eq. 26, the distance, *X* is obtained as,

$$X = \frac{H\sin(\theta-\delta)\cos\phi}{2\sin(\alpha_{cr}-\phi)\cos\delta\,\sin\alpha_{cr}} - \frac{H(\cot\alpha_{cr}-\cot\theta)[\cos(\theta-\delta)+\sin(\theta-\delta)\cot(\alpha_{cr}-\phi)]}{2\cos\delta} \quad (27)$$

The height of point of application of P_{aq} from the wall base, *h* is obtained as,

$$h = X\sin\theta \quad (28)$$

The coefficient of active earth pressure (K_{aq}) for the retaining wall with the surcharge effect is obtained as,

$$K_{aq} = \frac{P_{aq}}{\gamma H} \quad (29)$$

10. ACTIVE THRUST UNDER THE COMBINED EFFECT

In Table 1, the values of critical angle α_{cr} corresponding to the failure surface are reported, separately for the self-weight effect and the surcharge effect for various combinations of the parameters involved in the analysis. It is seen that, for any specified combination, the angle α_{cr} remains the same under the isolated effect of self-weight and surcharge. Therefore, the principle of superposition is valid in this case and the total active thrust, $P_{a\gamma q}$, under the combined effect of self-weight and surcharge is given as,

$$P_{a\gamma q} = P_{a\gamma} + P_{aq} \quad (30)$$

Table 1 Critical angle of failure surface, α_{cr} for both self-weight and surcharge effects with the combination of various parameters

Angle of wall back, θ (degrees)	Angle of soil friction, ϕ (degrees)	Angle of wall friction, δ (degrees)	Self-weight effect		Surcharge effect	
			$P_{a\gamma}$ (KN/m)	α_{cr} (degrees)	P_{aq} (KN/m)	α_{cr} (degrees)
85	28	18.67	0.358	56.6	0.507	56.6
80			0.4	58.3	0.566	58.35
75			0.447	59.893	0.633	59.893
70			0.502	61.339	0.71	61.339
65			0.566	62.636	0.800	62.636
85	30	20	0.334	57.779	0.473	57.779
80			0.376	59.489	0.532	59.489
75			0.424	61.058	0.6	61.058
70			0.479	62.51	0.677	62.51
65			0.543	63.8	0.768	63.8

11. POINT OF APPLICATION OF ACTIVE THRUST UNDER COMBINED EFFECT

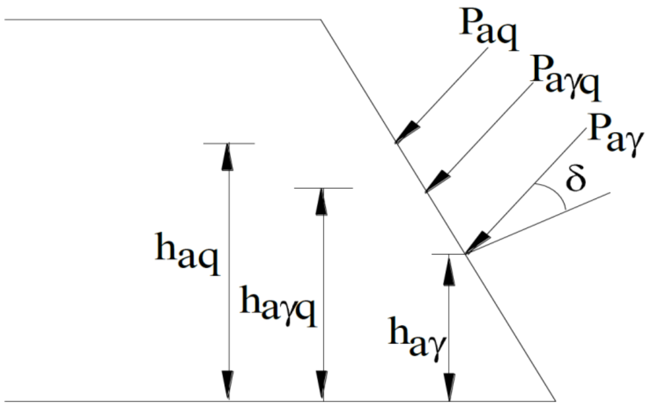

Fig. 6 Point of application of the active thrust from wall base

After knowing the active thrust due to the individual effect of self-weight and surcharge and its point of application from the wall base, condition of moment equilibrium is applied to determine the point of application of active thrust, $P_{a\gamma q}$ under the combined effect. Taking moment equilibrium condition about the base of the wall, the following expression is obtained.

$$h_{a\gamma q} = \frac{P_{aq} h_{aq} + P_{a\gamma} h_{a\gamma}}{P_{a\gamma q}} \quad (31)$$

Where, $h_{a\gamma q}$ is the distance of point of application of $P_{a\gamma q}$ from the wall base.

12. RESULTS AND DISCUSSIONS

The main aim of the proposed analysis is to determine the point of application of the active thrust under the combined effect of self-weight and surcharge. This result in terms of $h_{a\gamma q}$ is presented in a non-dimensional form, H_r, expressed as $h_{a\gamma q}/H$. The variations of H_r and the active thrust, $P_{a\gamma q}$ with various parameters are presented in the form of graphs and in Table 2 along with the discussions given below.

In Fig. 7, Fig. 8 and Fig. 9 are shown the variations of H_r with angle of soil friction, ϕ for δ = 2/3 ϕ, 1/3 ϕ and 0˚, respectively. It is seen that, H_r shows an increasing trend with increase in angle of soil friction, ϕ and a decreasing trend with increase in the angle of wall back, θ.

In Fig. 10, Fig. 11 and Fig. 12 are shown the variations of H_r with the angle of wall back, θ for δ = 0˚, 1/3 ϕ and 2/3 ϕ, respectively. It is seen that, H_r shows a decreasing trend with increase in the angle of wall back, θ, and an increasing trend with increasing angle of soil friction, ϕ.

In Fig. 13, variation of H_r with the angle of soil friction, ϕ is shown for a vertical retaining wall, angle of wall back, θ =

90˚ and angle of wall friction, δ = 0˚. It is interesting to note that, H_r has a constant value of 0.5 for all the values of angle of soil friction, ϕ. Hence, the point of application of active thrust acts at the mid-height of a smooth vertical retaining wall with horizontal backfill under the combined effect of surcharge and self-weight.

Table 2 Variations of H_r and $P_{a\gamma q}$ with angle of wall back, θ for angle of wall friction, δ = 0, 1/3 ϕ and 2/3 ϕ degrees

Angle of soil friction, ϕ (degrees)	Angle of wall back, θ (degrees)	Angle of wall friction, δ = 0˚		Angle of wall friction, δ=1/3 ϕ (degrees)		Angle of wall friction, δ=2/3 ϕ (degrees)	
		$P_{a\gamma q}$ (KN/m)	H_r	$P_{a\gamma q}$ (KN/m)	H_r	$P_{a\gamma q}$ (KN/m)	H_r
20	85	1.291	0.452	1.186	0.422	1.142	0.380
	80	1.349	0.476	1.278	0.447	1.239	0.408
	75	1.449	0.491	1.381	0.467	1.348	0.432
	70	1.562	0.503	1.500	0.481	1.474	0.449
	65	1.695	0.512	1.637	0.494	1.620	0.462
25	85	1.062	0.461	0.994	0.424	0.959	0.377
	80	1.154	0.487	1.088	0.456	1.060	0.412
	75	1.256	0.509	1.195	0.480	1.173	0.439
	70	1.372	0.522	1.316	0.498	1.303	0.461
	65	1.507	0.535	1.456	0.512	1.454	0.475
30	85	0.888	0.468	0.830	0.428	0.807	0.379
	80	0.981	0.500	0.925	0.466	0.908	0.419
	75	1.084	0.525	1.031	0.495	1.024	0.450
	70	1.201	0.545	1.154	0.516	1.156	0.473
	65	1.335	0.557	1.294	0.532	1.311	0.489
35	85	0.737	0.478	0.689	0.435	0.679	0.379
	80	0.827	0.515	0.783	0.479	0.780	0.428
	75	0.93	0.542	0.889	0.512	0.895	0.465
	70	1.046	0.566	1.009	0.537	1.029	0.490
	65	1.178	0.580	1.149	0.554	1.186	0.506
40	85	0.604	0.485	0.568	0.443	0.569	0.387
	80	0.693	0.532	0.659	0.493	0.669	0.441
	75	0.792	0.564	0.762	0.532	0.783	0.481
	70	0.905	0.589	0.881	0.559	0.918	0.509
	65	1.034	0.607	1.019	0.576	1.077	0.524

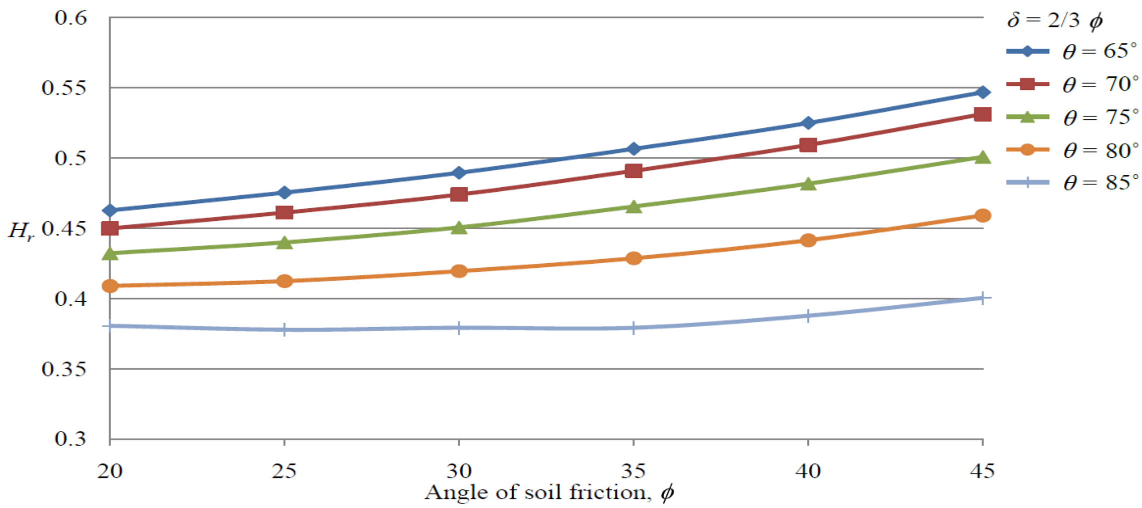

Fig. 7 Variation of Hr with angle of soil friction, ϕ

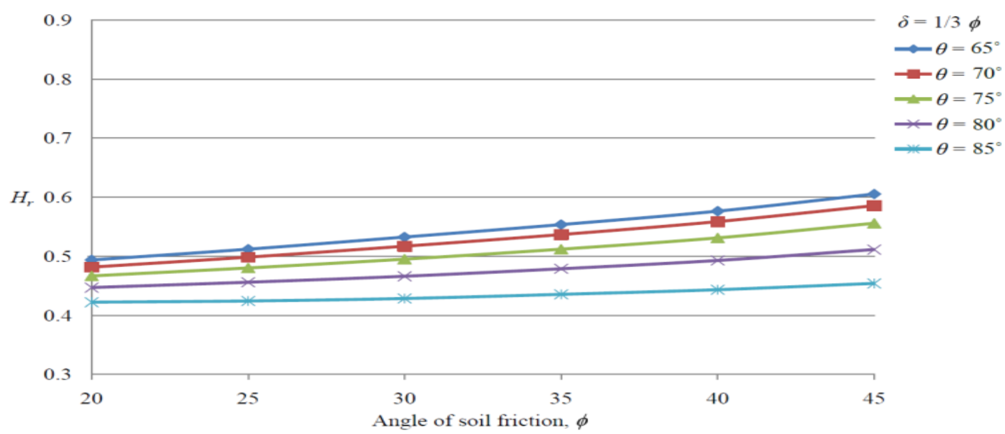

Fig. 8 Variation of Hr with angle of soil friction, ϕ

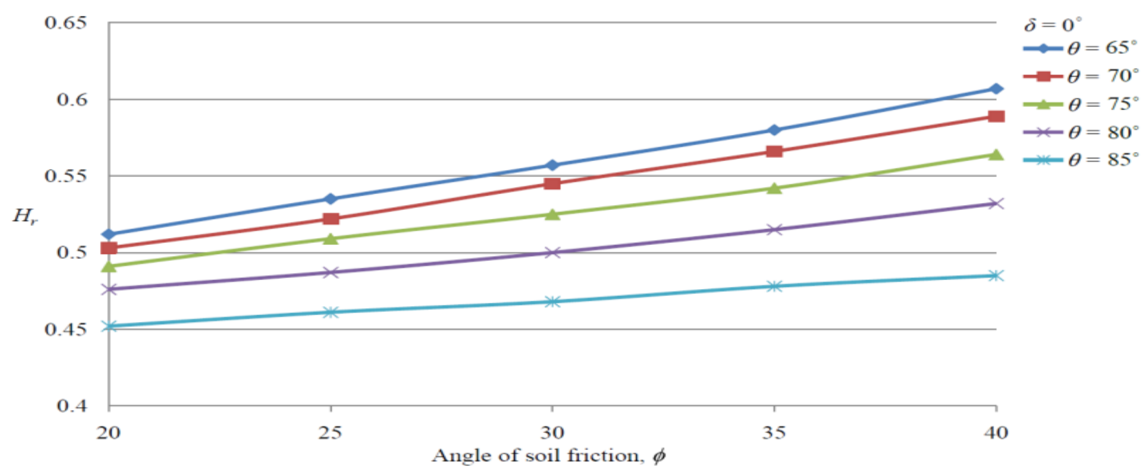

Fig. 9 Variation of Hr with angle of soil friction, ϕ

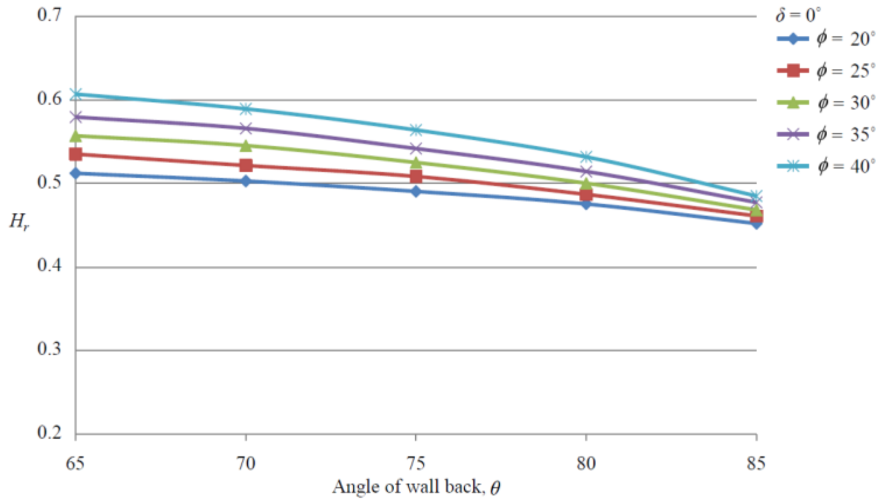

Fig. 10 Variation of Hr with angle of wall back, θ

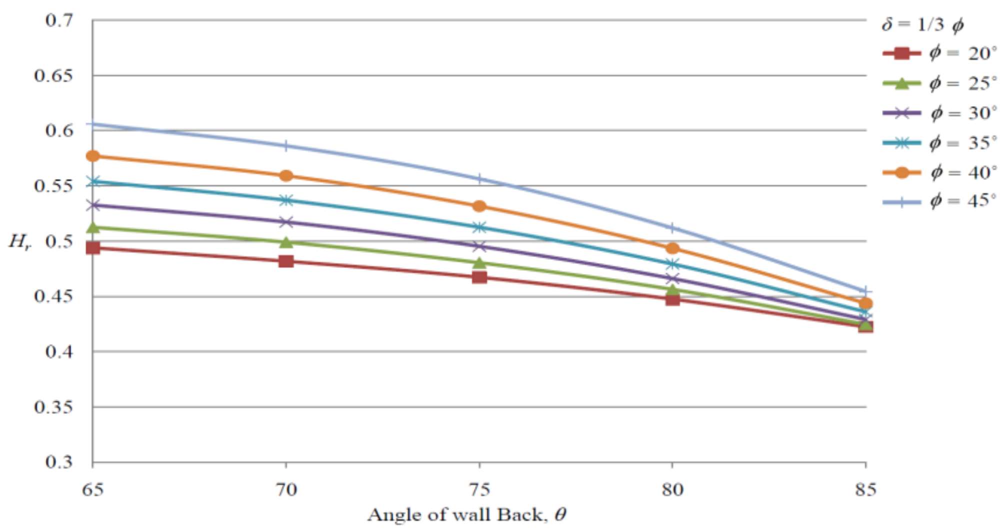

Fig. 11 Variation of Hr with angle of wall back, θ

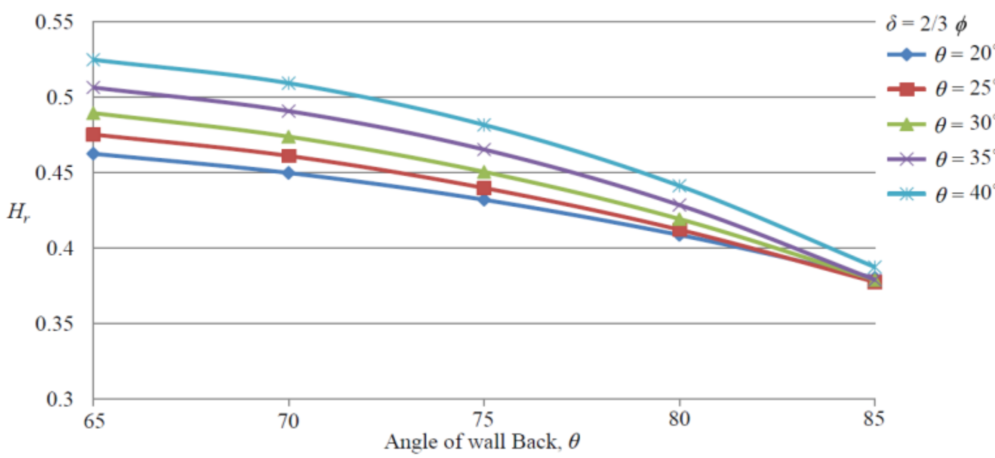

Fig. 12 Variation of Hr with angle of wall back, θ

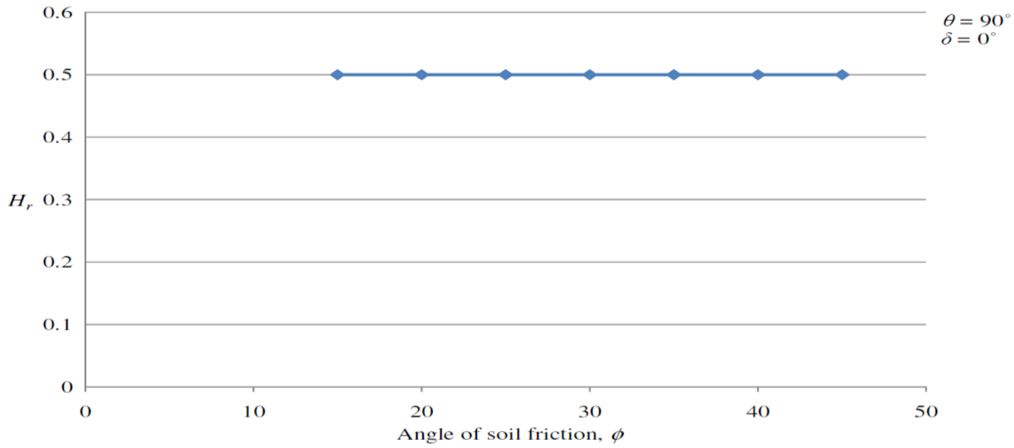

Fig. 13 Variation of H_r with soil friction angle, ϕ

12. CONCLUSIONS

The active thrust and its point of application under the combined effect of self-weight and surcharge for an inclined wall with horizontal cohesionless backfill are computed using all the conditions of equilibrium along with the principle of superposition. The proposed analysis effectively uses Kötter's (1903) equation to determine the reactive pressure distribution on the failure plane. It is seen that, the point of application of the active thrust depends upon several factors such as angle of soil friction, ϕ, angle of wall friction, δ, and angle of wall back, θ. It shows a wide variation in the range, 0.534 to 0.773. For a vertical smooth wall under the effect of surcharge and self-weight the active thrust acts at the mid-height of the wall.

REFERENCES

Caquot AI, Kerisel J (1948) Tables for the calculation of passive pressure, active pressure, and bearing capacity of foundations. Libraire du Bureau des Longitudes, de L'ecolePolytechnique, Paris Gauthier- villars, Imprimeur- Editeur, 120
Chen Z, Li S (1998) Evaluation of active earth pressure by the generalized method of slices. Canadian Geotechnical Journal, 35: 591-599
Ching S, Sao J (1994) Discrete element analysis for active and passive pressure distribution on retaining wall. Computers and Geotechnics, 16: 291-310
Coulomb CA (1776) Essaisurune application des règles des maximis et minimis à quelquesproblèmes de statiquerelatifs à l'architecture. Mèm. Acad. Roy. Près. Divers Savants 7, Paris
Dewaikar DM, Halkude SA (2002) Seismic passive/active thrust on retaining wall- point of application. Soils andFoundations, 42(1): 9-15
Janbu N (1957) Earth pressure and bearing capacity calculations by generalized procedure of slices. Proc. of 4th International Conference on Soil Mechanics and Foundation Engineering, London, 2, pp. 207-212
Kame GS, Dewaikar DM, Choudhury D (2010) Active Thrust on a Vertical Retaining Wall with Cohesionless Backfill. Electronic Journal of Geotechnical Engineering, 15(Q): 1848-1863
Kérisel J, Absi E (1990) Tables de poussée et de butée des terres. 3rd ed., Presses del' E´cole Nationale des Pontset Chaussées, Paris, 1990
Kötter F (1903) Die Bestimmung des Drucks an gekrümmten Gleitflächen, eine Aufgabe aus der Lehre vom Erddruck. Sitzungsberichte der Akademie der Wissenschaften, Berlin, pp. 229-233. Lancellotta R (2002) Analytical solution of passive earth pressure. Géotechnique, 52(8): 617-619
Rahardjo H, Fredlund, DG (1984) General limit equilibrium method for lateral earth force. Canadian Geotechnical Journal, 21: 166-175
Rankine WJM (1857) On the stability of loose earth. Philosophical Transactions of the Royal Society, London, vol.147
Sokolovski VV (1960) Statics of Soil Media. Butterworth Publications, London
Soubra AH, Macuh B (2002) Active and passive earth pressure coefficients by a kinematical approach. Proc. of the Institution of Civil Engineers Geotechnical Engineering, 2, pp. 119-131
Wang YZ (2000) Distribution of earth pressure on a retaining wall. Géotechnique 50(1): 83-88